

AUTOMATED DETECTION AND MONITORING OF GLIDE-SNOW EVENTS USING SATELLITE-BASED OPTICAL REMOTE SENSING AND TERRESTRIAL PHOTOGRAPHY

Sebastian Feick^{1*}, Christoph Mitterer², Lisa Dreier², Stephan Harvey², Jürg Schweizer²

¹ Institute of Geography, University of Erlangen-Nürnberg, Germany

² WSL Institute for Snow and Avalanche Research SLF, Davos, Switzerland

ABSTRACT: On steep slopes the full snowpack can glide on the ground, tension cracks may open and eventually the slope fails as full-depth avalanche (glide-snow avalanche). Many observations have shown that a thin wet layer reduces friction between the snow-soil interface leading to snow gliding. The occurrence, however, of glide cracks and their evolution to glide avalanches are still poorly understood. Permanent monitoring of glide cracks seems most promising for predicting snow gliding and full-depth avalanches. We evaluated whether glide cracks can be automatically detected and mapped for a large area using optical satellite images with very high spatial resolution. Two approaches were tested for a 25 km² scene from panchromatic satellite sensor WorldView-1 acquired over a test site in the Eastern Swiss Alps. Both approaches integrate image information and topographic variables derived from a digital elevation model. The first approach is based on statistical modeling techniques; the second one included an object-based image analysis. Both approaches achieved encouraging detection and mapping accuracies even though certain limitations exist. Furthermore, images from temporal high resolution time-lapse photography of two slopes that are known for gliding-snow events were used to monitor glide-crack evolution and glide-avalanche occurrence.

1. INTRODUCTION

Glide-snow avalanches are a recurring challenge for avalanche warning services and avalanche control programs in many snow climates (Simenhois and Birkeland, 2010; Peitzsch et al., 2012). Numerous observations suggest that a thin wet layer reduces friction between the snow-soil interface leading to gliding of the full snowpack on the ground (In der Gand and Zupancic, 1966; Lackinger, 1987; Clarke and McClung, 1999). Tension cracks may open when glide rates vary on a slope and eventually the slope may fail as a full-depth avalanche. The occurrence, however, of glide cracks and their evolution into glide-snow avalanches is still poorly understood. Liquid water in combination with terrain and snowpack properties is assumed to play a major role for snow gliding processes (Jones, 2004; Reardon et al., 2006). Different sources for liquid water at the snow-soil interface exist. Depending on weather, snow cover and soil conditions either basal melting due to heat flux from the ground, water infiltration due to rain or surface melting predominates.

Glide-snow avalanches were observed to occur in an almost entirely dry as well as in an entirely wet snowpack. A strong correlation exists to

terrain features. Glide cracks often develop at similar slope positions; only in specific starting zones they develop into glide avalanches (Lackinger, 1988). In addition, limited control possibilities make glide-snow avalanches highly unpredictable (Reardon et al., 2006). Peitzsch et al. (2012) achieved promising forecasting results for glide-avalanche occurrence in spring, i.e. for conditions when the snowpack had reached an isothermal state and infiltrating water penetrated the entire snowpack. They did not observe avalanches when the snowpack was still dry. Clarke and McClung (1999) call these avalanches cold-temperature events and conclude that they are the most difficult type of glide-snow events to forecast.

To improve forecasting a better knowledge of the processes dominating snow gliding needs to be developed. This requires continuous glide monitoring. A number of studies dealt with methods to measure glide rates or methods to detect and monitor glide-snow events (In der Gand, 1957; Akitaya, 1980; McClung et al., 1994; Wilson et al. 1996; Stemberis and Rubin, 2005; Hendrikx et al., 2010; van Herwijnen and Simenhois, 2012). In all of these studies gliding was monitored at one or only a few specific slopes. Today, remote sensing instruments, especially satellite based, are able to acquire data of large areas without the restriction of poor ground accessibility. Bühler et al. (2009) developed an approach for wide-area detection and mapping of snow avalanche deposits based on data acquired by an airborne multiangular sensor. A new generation of optical satellite sensors

Corresponding author address: Sebastian Feick,
Institute of Geography, Kochstrasse 4,
D-91054 Erlangen, Germany
tel: +49 9131 85 22016; fax: +49 9131 85 22016
email: sfeick@geographie.uni-erlangen.de



Figure 1: Monitored slopes (summer and winter) at Chüenihorn above St. Antönien (Switzerland).

achieves spatial resolutions of less than 1 m offering a comparable resolution to aerial scans. Satellite remote sensing is characterized by wide-area scans, frequent revisiting times and lower costs compared to airborne remote sensing.

We used spatially very high-resolution satellite images (WorldView-1; DigitalGlobe, 2009) for systematically detecting and mapping glide cracks and glide-snow avalanches. Today satellite revisiting times are not adequate to monitor glide-crack evolution in detail and to determine the time of release (WorldView-1 average revisiting time: 2-5 days). For this purpose terrestrial time-lapse photography was used to complete the data set.

2. DATA AND METHODS

2.1 *Automated detection of glide cracks*

A 25 km² WorldView-1 sensor satellite scene recorded on 28 April 2008 over the valley of St. Antönien (Eastern Swiss Alps) formed the basis for testing different glide-crack detection algorithms. We have chosen this scene as the valley of St. Antönien is known for its glide-snow activity. Large areas covered by steep meadows and pastures (parent rock material is flysch) provide favorable conditions for the formation of glide cracks.

WorldView-1 sensor is an optical and panchromatic satellite sensor with a spatial resolution of 0.5 m at nadir. Additionally a 2 m digital elevation model (DEM), resampled to 0.5 m resolution, and a vector data set (Swisstopo, 2010) including land cover information were acquired. First glide cracks were manually digitized from the satellite image as reference data set. Then areas unlikely for glide-crack occurrence, i.e. very flat and very steep areas, closed forest stands and urban areas, were excluded by masking. Finally, based on image grey scale values and several topographic variables derived from the DEM two approaches were tested to automatically detect glide cracks.

The first approach included statistical modeling using a generalized additive model (GAM). The GAM is a semi-parametric extension of logistic regression that allows modeling both linear and nonlinear influences of predictor variables on the binomial response (Hastie and Tibshirani, 1990), here the presence ($Y = 1$) or absence ($Y = 0$) of glide crack pixels. A stepwise forward selection based on the Akaike Information Criterion (AIC; Bozdogan, 1987) is applied to decide whether a variable is included as a transformed additive effect, a linear effect, or omitted. In recent years, the capability of GAM in the field of geomorphological distribution modeling in complex terrain was demonstrated and it has been proven to be competitive with some highly flexible machine-learning techniques (e.g. Brenning, 2005; 2009; Park and Chi, 2008).

The second approach included an object-based image analyzing (OBIA) method. On the basis of a homogeneity criterion, object-oriented classification methods merge adjacent pixels to image segments. Further parameters such as topological, shape and statistical information allocate these image segments as objects to a predefined class hierarchy. Detailed overviews of object-oriented image analyzing and a comparison to pixel based approaches are given by e.g. Benz et al. (2004) and Dehvari and Heck (2009). Bühlert et al. (2009) used object-oriented classification in their processing chain for an automated detection of avalanche deposits achieving promising mapping results.

Finally, image classification accuracy was assessed based on quantitative measures derived from confusion matrices to analyze and compare the results of both processing chains. Foody (2010, 2011) gives a detailed introduction to accuracy assessment in remote sensing using confusion matrices. Due to the limited dimension of the satellite scene (25 km²) we did not distinguish

between training and test data sets. Thus, results are biased towards too optimistic values.

2.2 Monitoring glide-snow events

Temporal high resolution time-lapse photography (15 min intervals) of two slopes that are known for glide-snow events were used to monitor glide-crack evolution and avalanche occurrence. One camera was located near St. Antönien taking pictures of the mostly steep to very steep south-east facing slopes of Chüenihorn (2413 m a.s.l.). Slopes are mainly covered by meadows interspersed with closed and open forest stands (Fig. 1). Monitored elevations are in the range of 1500 m to 2250 m above sea level. The second camera is installed on a building in Davos viewing parts of the Dorfberg (main peak is Salezer Horn, 2536 m a.s.l.). The monitored area ranges from 1700 m to 2400 m above see level. Aspects are predominately east-south-east facing and land cover mostly consists of steep to very steep meadows but also some rocky areas and parts with closed or open forest stands and shrubberies exist. Standard photo cameras recording pictures in the visible light spectrum were used which means that we were depending on visibility. During night or periods with low visibility due to bad weather conditions no or incomplete information could be recorded. The camera positions towards the slopes were oblique.

The winter 2011-2012 had an above average glide-snow activity. The analyzed periods last from 8 December 2011 through 9 March 2012 at the site Davos and from 19 December 2011 through 9 March 2012 at the site St. Antönien. Each photo was manually analyzed gathering several variables (Table 1). On both study sites snow gliding was the predominately underlying process for full-depth avalanches ensuring almost certainly a classification as glide snow avalanche also in cas-

es when no glide crack could be identified before a full-depth release occurred.

Table 1: Attributes extracted from manual photo analysis.

Glide cracks	Glide-snow avalanches
Date	Date
Time	Time
Initial opening at night	Released at night
Remarkable widening before release	Above glide crack or avalanche

3. RESULTS AND DISCUSSION

3.1 Automated detection of glide cracks

The panchromatic WorldView-1 image was suitable for manual glide-crack detection. Glide cracks could be clearly identified in the vast majority of cases. However, artificial pixel coarsening exhibited that a spatial resolution better than 1 m is necessary. Also other relevant phenomena such as (dry-snow) slab or loose-snow avalanches, avalanche deposits or snow dunes were well visible. Some problems resulted from the late recording date (28 April 2008). Many of the south-facing slopes had already been released and were snow-free. However, more than 1,000 glide cracks and glide-snow avalanche starting zones were manually digitized as reference data set.

Results for both processing chains (statistical modeling and object-based image analyses) are presented in the confusion matrices of Table 2. The sensitivity, i.e. the proportion of glide crack pixels correctly classified to all glide crack pixels observed, was similarly high for the two approaches: 81% and 78% respectively. The specificity, i.e. the proportion of non-glide crack pixels correctly classified to all non-glide crack pixels observed,

Table 2: Confusion matrices representing numbers of observed (manually digitized) and predicted pixels classified as glide crack or non-event areas. Results (not cross-validated) are presented for the statistical modeling approach (GAM) and the approach containing the object-based image analyzes (OBIA).

Predicted	Observed			
	GAM		OBIA	
	1	0	1	0
1	143,526	2,991,544	138,640	3,804,216
0	34,619	92,078,747	39,505	91,266,075

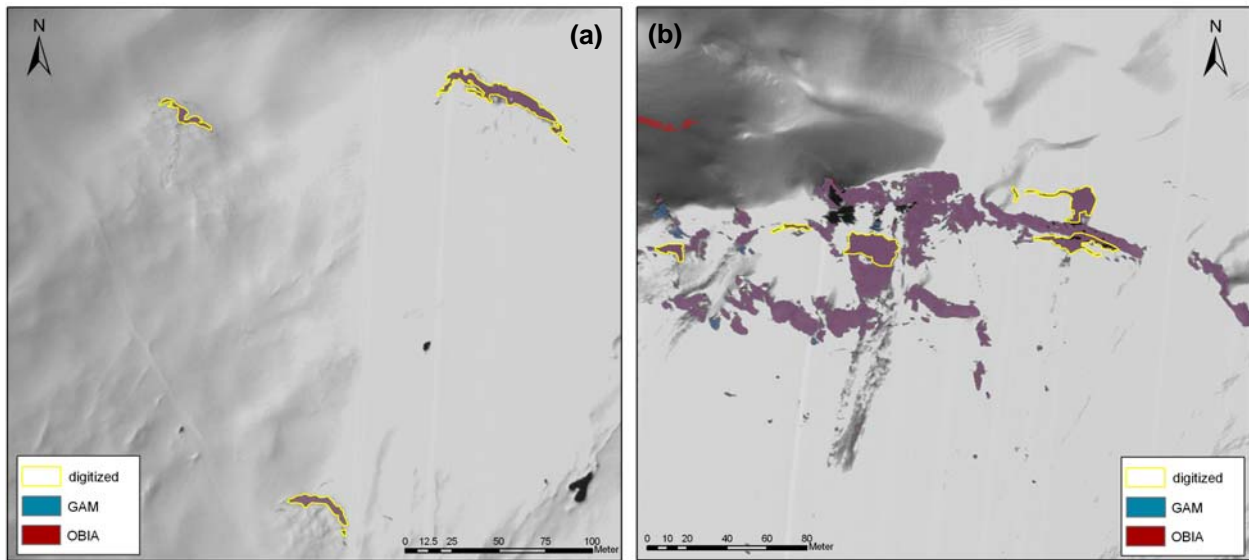


Figure 2: (a) Glide cracks on completely snow-covered slopes are mapped with high accuracies; (b) Misclassifications occurred in rocky and steep snow free areas. Pixels modeled from both approaches as glide crack pixels are purple colored because used colors (red and blue) have a 50% transparency.

was even very high: 97% and 96% respectively. The true skill score was 77% for the GAM approach and 74% for the OBIA approach. However, the high false alarm ratios of 95% and 96%, respectively, point to the main classification problem. Both classification approaches considerably overestimated glide-crack areas. Glide cracks within completely snow-covered slopes were mapped with high accuracy (Fig. 2a). Misclassifications occurred particularly in rocky areas, areas with single tree stands or in starting zones with supporting structures and in already avalanche-affected, steep snow-free areas (Fig. 2b). As mentioned results are not cross-validated.

An improved masking of the satellite image excluding single tree stands, supporting structures and some of the rock areas should lead to better classification results in the future. As glide-snow avalanches can occur even on rocks not all of them can be excluded in general. As mentioned above many starting zones already had released; these mainly south-facing slopes had large areas which were snow-free. These steep snow-free areas were also mapped as glide-crack areas contributing to the high error rates of the predictive positive value.

3.2 Monitoring glide-snow events

Based on the terrestrial photo archive 146 glide cracks and 101 full-depth avalanches were manually detected in the 2011-2012 season at Davos (Fig. 3). At St. Antönien 246 glide cracks

and 303 glide-snow avalanches were identified. About 10-25% of the crack openings and glide avalanches occurred at night. Only about 40% of the glide cracks resulted into glide-snow avalanches. For 41% and 55% of the glide-snow avalanches in Davos and St. Antönien, respectively, no glide-crack opening could be identified in one of the previous photos. This high proportion is partly due to the relatively large distance between the cameras and some parts of the investigated slopes, the flat angle of incidence between camera position and slope and the relatively large time-lapse interval (15 min). The mentioned shortcomings could also lead to the low percentage (about 30%) of glide cracks that significantly widened before a glide avalanche released. However, Simenhois and Birkeland (2010) also reported glide avalanches before new glide cracks were observed. Surprisingly, about every tenth full-depth avalanche occurred directly above and not below a glide crack or an already released glide avalanche which was to our knowledge only reported by Lackinger (1988). Most glide-crack openings and glide avalanches were observed in the time period between 11:15 and 14:30 ("noon"; Fig. 3). This diurnal cycle is evident for all full-depth avalanches as well as for the avalanches following the opening of a glide crack (i.e. obvious glide-snow avalanches). Furthermore, a diurnal cycle was observed independently of the type of snow gliding, i.e. when the majority of the snowpack was still dry as well as when the snowpack was isothermal and wet.

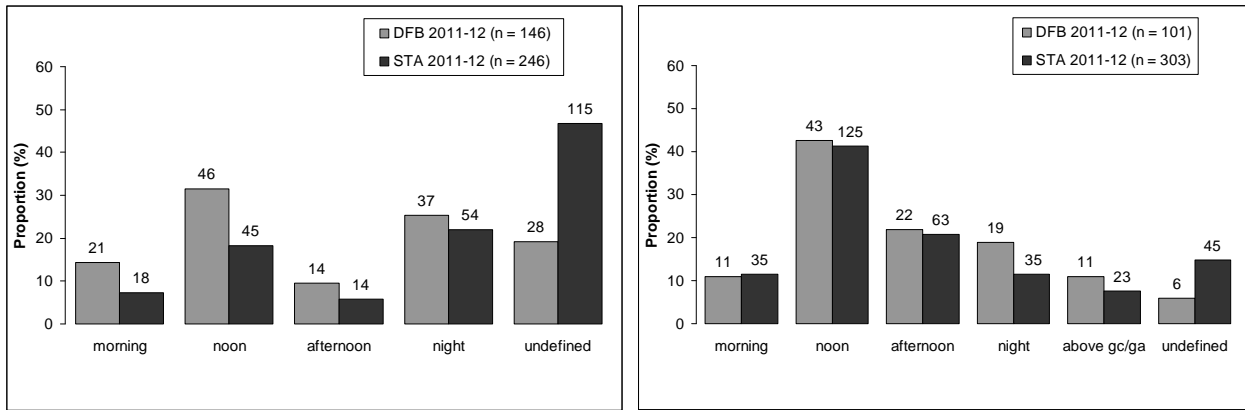


Figure 3: (a) Glide crack and (b) glide avalanche occurrence (time of day) from two series of time-lapse photographs. Height of bars is proportion (%) of all events per winter and site. The number on top of the bar indicates the number of cases. “Above gc/ga” indicates cases where a glide avalanche occurred directly above and not below a glide crack or an already released glide avalanche (DFB = Dorfberg; STA = St. Antönien).

In relation to the analysis of the time-lags between initial crack opening and the resulting avalanche it has to be mentioned that the point of initial crack opening and the point of glide-avalanche release refers to the first photo on which a crack or avalanche could be identified. Thus, for a few cases the recorded time lags were either too short, i.e. cases when glide cracks opened in periods with no visibility (night, poor weather conditions) or too long, i.e. cases when glide-snow avalanches occurred in periods with no visibility (night, poor weather conditions). However, nearly 15% of the glide cracks avalanched within the first hour and 40% within the first 5 hours after crack opening. About 80-90% avalanched within 12-72 hours. These values and the high percentage of glide-snow avalanches without identifiable previous crack opening mentioned above suggest that (very) short time lags between initial crack opening and subsequent glide-snow avalanching are common.

4. CONCLUSIONS

Spatially very high resolution satellite images proved to be suitable for manual glide-crack detection. Both automated modeling approaches mapped glide cracks on completely snow-covered slopes with high accuracy. Limitations exist in terms of over-estimating glide crack pixels in rocky areas, areas with single tree stands or supporting structures and in steep snow-free areas. The statistical modeling approach performed slightly better than the object-oriented classification ap-

proach. In addition, it offers more flexible model development capabilities for future work.

Analyzing the terrestrial photographs suggests that the majority of glide cracks never developed into an avalanche. Nearly 15% of glide cracks resulted in an avalanche releasing within the first hour and 40% within the first 5 hours after crack opening. In many cases it was not possible to identify the crack opening in the photo preceding the glide-snow avalanche release. Whether in fact, glide-snow avalanches frequently occur without a delay between crack opening and release, could not be fully clarified. However, (very) short time lags between initial crack opening and subsequent glide avalanching are certainly typical. Glide-snow activity had a clear diurnal cycle with most events occurring at noon.

In the future, we will relate glide crack and avalanche occurrence to meteorological and terrain parameters. Also, we will acquire new satellite images to test the modeling approaches and get reliable error rates. Excluding obvious areas of misclassification from the satellite images by improved masking should lead to better classification results. However, a prerequisite for an improved masking and for multi-temporal change detection is an accurate satellite image orthorectification which poses a challenge in snow-covered alpine terrain. Even though satellite images currently are not adequate to monitor glide cracks due to limited temporal resolution, we see great potential in using remote sensing for snow and avalanche applications in the future.

ACKNOWLEDGMENTS

We thank Anna Haberkorn, Ariane Steubli, Benjamin Reuter, Stephan Simioni and Lino Schmid for help with acquiring the time-lapse photographs.

REFERENCES

- Akitaya, E., 1980. Observations of ground avalanches with a video tape recorder (VTR). *J. Glaciol.*, 26(94): 493-496.
- Benz, U.C., Hofmann, P., Willhauck, G., Lingenfelder, I., Heyen, M., 2004. Multi-resolution, object-oriented fuzzy analysis of remote sensing data for GIS-ready information. *ISPRS J. Photogramm.*, 58: 239-258.
- Bozdogan, H., 1987. Model selection and Akaike's Information Criterion (AIC): The general theory and its analytical extensions. *Psychometrika*, 52(3): 345-370.
- Brenning, A., 2009. Benchmarking classifiers to optimally integrate terrain analysis and multispectral remote sensing in automatic rock glacier detection. *Remote Sens. Environ.*, 113: 239-247.
- Brenning, A., 2005. Spatial prediction models for landslide hazards: Review, comparison and evaluation. *Nat. Hazard. Earth Sys.*, 5(6): 853-862.
- Bühler, Y., Hüni, A., Christen, M., Meister, R. and Kellenberger, T., 2009. Automated detection and mapping of avalanche deposits using airborne optical remote sensing data. *Cold Reg. Sci. Technol.*, 57(2-3): 99-106.
- Clarke, J. and McClung, D.M., 1999. Full-depth avalanche occurrences caused by snow gliding, Coquihalla, British Columbia, Canada. *J. Glaciol.*, 45(151): 539-546.
- Dehvari, A. and Heck, R.J., 2009. Comparison of object-based and pixel based infrared airborne image classification methods using DEM thematic layer. *Journal of Geography and Regional Planning*, 2(4): 86-96.
- DigitalGlobe, 2009. Satellite Imagery and Geospatial Information Products. www.digitalglobe.com.
- Foody, G.M., 2011. Classification accuracy assessment. *IEEE Geoscience and Remote Sensing Newsletter*, 159: 8-14.
- Foody, G. M., 2010. Assessing the accuracy of land cover change with imperfect ground reference data. *Remote Sens. Environ.*, 114: 2271-2285.
- Hastie, T. and Tibshirani, R., 1990. Generalized additive models. CRC Press, Boca Raton, Florida.
- Hendrikx, J., Peitzsch, E. and Fagre, D.B., 2010. A practitioner's tool for assessing glide crack activity, International Snow Science Workshop ISSW, Lake Tahoe CA, U.S.A., 17-22 October 2010, pp. 395-396.
- in der Gand, H.R. and Zupancic, M., 1966. Snow gliding and avalanches, Symposium at Davos 1965 - Scientific Aspects of Snow and Ice Avalanches, IAHS Publication, 69. Int. Assoc. Hydrol. Sci., Wallingford, U.K., pp. 230-242.
- in der Gand, H.R., 1957. Ergebnisse der Gleitmessung. In: M. de Quervain (Editor), Schnee und Lawinen in den Schweizeralpen, Winter 1955/1956 - Winterbericht des Eidg. Institutes für Schnee- und Lawinenforschung, No. 20. Eidg. Institut für Schnee- und Lawinenforschung, Weissfluhjoch/Davos, pp. 111-114.
- Jones, A., 2004. Review of glide processes and glide avalanche release. *Avalanche News*, 69: 53-60.
- Lackinger, B., 1988. Zum Problem der Gleitschneelawine. In: G. Fiebiger and F. Zollinger (Editors), Interpraevent 1988, Graz, Austria, pp. 205-226.
- Lackinger, B., 1987. Stability and fracture of the snow pack for glide avalanches. In: B. Salm and H. Gubler (Editors), Symposium at Davos 1986 - Avalanche Formation, Movement and Effects, IAHS Publ., 162. International Association of Hydrological Sciences, Wallingford, Oxfordshire, U.K., pp. 229-241.
- McClung, D.M., Walker, S., Golley, W., 1994. Characteristics of snow gliding on rock. *Ann. Glaciol.* 19: 97-103.
- Park, N.W. and Chi, K.H., 2008. Quantitative assessment of landslide susceptibility using high-resolution remote sensing data and a generalized additive model. *Int. J. Remote Sens.*, 29(1): 247-264.
- Peitzsch E.H., Hendrikx J., Fagre D.B., Reardon, B., 2012. Examining spring wet slab and glide avalanche occurrence along the Going-To-The-Sun Road corridor, Glacier National Park, Montana, USA. *Cold Reg. Sci. Technol.*, 78: 73-81.
- Reardon, B., Fagre, D.B., Dundas, M., Lundy, C., 2006. Natural glide slab avalanches, Glacier National Park, U.S.A.: A unique forecasting challenge. In: Gleason, J.A. (Editor), Proceedings ISSW 2006, Telluride, CO, U.S.A., pp. 778-785.
- Simenhois, R. and Birkeland, K., 2010. Meteorological and environmental observations from three glide avalanche cycles and the resulting hazard management technique, International Snow Science Workshop ISSW, Lake Tahoe

- CA, U.S.A., 17-22 October 2010, pp. 846-853.
- Stimberis, J. and Rubin, C., 2005. Glide avalanche detection on a smooth rock slope, Snoqualmie Pass, Washington. In: K. Elder (Editor), Proceedings ISSW 2004. International Snow Science Workshop, Jackson Hole WY, U.S.A., 19-24 September 2004, pp. 608-610.
- Swisstopo, 2010. VECTOR25. Das digitale Landschaftsmodell der Schweiz, Bundesamt für Landestopographie.
- van Herwijnen, A. and Simenhois, R., 2012. Monitoring glide avalanches using time-lapse photography, International Snow Science Workshop ISSW 2012, Anchorage AK, U.S.A., 16-21 September 2012, pp. in press (see this issue).
- Wilson, A., Statham, G., Bilak, R. and Allen, B., 1997. Glide avalanche forecasting, Proceedings International Snow Science Workshop, Banff, Alberta, Canada, 6-10 October 1996. Canadian Avalanche Association, Revelstoke BC, Canada, pp. 200-202.